

Hopping conduction in semiconducting diamond

B. Massarani* and J. C. Bourgoin

Groupe de Physique des Solides de l'École Normale Supérieure, Université Paris VII, Tour 23, 2 Place Jussieu, 75221 Paris Cedex 05, France

R. M. Chrenko

General Electric Research and Development Center, Schenectady, New York 12301

(Received 17 March 1977)

The electronic conductivity of synthetic boron-doped diamonds is studied in the temperature range 12–1300°K. It is shown that in the low-temperature range (below 150–100°K) the results are best interpreted in terms of variable-range hopping. An attempt to evaluate quantitatively the parameters which characterize this hopping mechanism is made using the boron concentration and the degree of compensation determined from the variation of conductivity in the high-temperature range, coupled with optical-absorption measurements. The effect of irradiation with energetic electrons, which introduced new compensating centers, is investigated and can also be explained in terms of the theory for the hopping mechanism.

I. INTRODUCTION

At sufficiently low temperatures, electrical conduction in doped semiconductors is dominated by hopping of charge carriers between impurity centers when these impurity centers are partially compensated; this hopping conduction is made possible by the finite overlap of the wave functions of adjacent centers. There are several hopping mechanisms depending on the temperature range, the magnitude of the overlap of the wave functions, and the impurity bandwidth.¹

Semiconducting diamond represents in principle an ideal system for studying hopping conduction in a crystalline material. Indeed, due to the depth of the boron acceptor level E_A (0.37 eV above the valence band²⁻⁵), the conduction in the valence band becomes negligible at relatively high temperatures (150–200°K) and the hopping conduction can thus be studied in a very large temperature range (up to 200°K). Also, the Bohr radius of the ground state of the doping impurity is so small (around 3.5×10^{-8} cm when a hydrogenic model for the hole bound of the boron impurity is assumed) that impurity concentrations as high as 10^{20} cm⁻³ do not result in a metallic conduction. Such high concentrations induce a large impurity bandwidth (0.2 eV for a concentration of 10^{20} cm⁻³), corresponding to a large spread in the energy of the localized states of the impurity centers, which makes it possible to observe at a relatively high temperature the transition between the two hopping regimes: hopping through nearest-neighbor centers (NNH) and hopping through more distant impurity centers (VRH or variable range hopping). In other crystalline materials, this transition temperature is very low because the impurity bandwidth is very small (only few meV) even for

relatively high impurity concentrations (which do not render the conduction metallic). Transition temperatures of 1°K have been observed in germanium⁶ (doped with 2×10^{17} cm⁻³ Sb and compensated to 25%) and in *n*-type gallium arsenide⁷ (doped with 7×10^{15} cm⁻³ and compensated to 30%). Only in the case of heavily neutron-irradiated gallium arsenide⁸ has a significantly higher transition temperature (190°K) been reported; Coates and Mitchell⁸ suggested that, in this case, tunneling takes place between defect states, spread over nearly 100 meV, in concentration of about 8×10^{17} cm⁻³.

In previous works on boron-doped diamonds, electrical conductivity has been measured in natural as well as synthetic type-IIb crystals, down to 80°K,^{4,5,9-13} and it has been noticed^{12,13} that this conductivity is of hopping type for the lowest temperatures studied. The hopping conduction can occur when some of the boron acceptor centers are compensated by deep donor impurities such as substitutional nitrogen or by defects whose nature is unknown.

The aim of this paper is to study the hopping regime in boron-doped synthetic diamonds grown by General Electric. To perform such a study we had first to determine the boron concentration N_A and the concentration of the compensating centers N_D . We therefore studied the conductivity of the samples in the range 12–1000°K. Conductivity measurements at high temperatures, coupled with optical-absorption measurements, are used to determine N_A and N_D ; conductivity measurements at low temperatures are used to study the hopping mechanism. The knowledge of N_A , N_D , and of the compensation $K = N_D/N_A$ allows us to calculate the parameters which characterize this hopping mechanism. We also performed electron irradiation

tions, which introduce donor defects¹⁴ (i.e., new compensating centers), in order to study the variations of conductivity in the hopping range with changes in N_D and to verify that these variations can be accounted for by the hopping mechanism. Section II is devoted to a short description of the samples used and of the experimental set-up. The experimental results, concerning the variation of the conductivity $\sigma(T)$ in the low- and high-temperature ranges, and the effect of electron irradiation on $\sigma(T)$, are described in Sec. III. The concentrations N_A and N_D are deduced from $\sigma(T)$ in the high-temperature range in Sec. IV. Then, in Sec. V, we determine to what extent the results of $\sigma(T)$ in the low-temperature range can be accounted for by the existing theories of hopping conduction and we deduce the operative hopping regime. Finally, in Sec. VI, we calculate the values of the different parameters which characterize this hopping regime.

II. EXPERIMENTAL DETAILS

A. The samples

The samples used are boron-doped synthetic diamonds grown by General Electric. They have various sizes (typically $1 \times 1 \times 1$ mm up to $4 \times 3 \times 2$ mm) and irregular shapes. These diamonds contained not only boron, but also some macroscopic inclusions introduced during the growing process, and may be twinned. Details on their characteristics as well as on the growing procedure can be found elsewhere.^{2, 5, 15-17}

B. Measurements at low temperature

The samples are placed in a liquid-helium cryostat equipped with a temperature stabilizer¹⁸ (0.1 °K below 100 °K and 0.5 °K above) in the temperature range 4.2–360 °K. The sample holder has been designed in order to allow both good thermal contact with the helium exchange tube of the cryostat and good electrical insulation (the impedance of the sample to be measured can be $10^{15} \Omega$). The sample is pressed between an oxygen-free high-conductivity copper block (which is the bottom of the exchange tube and the electrical ground) and an insulating sapphire disk (Fig. 1). We verified that the electron irradiations did not significantly alter the electrical insulation of this disk. The sample temperature is measured with the aid of two thermocouples (a 0.03-at. % iron-doped gold-chromel thermocouple in the range 4.2–77 °K and a chromel-constant thermocouple in the range 77–360 °K). The conductivity is measured at constant voltage (a 1.35-V mercury cell) using an electrometer. In the lowest temperature

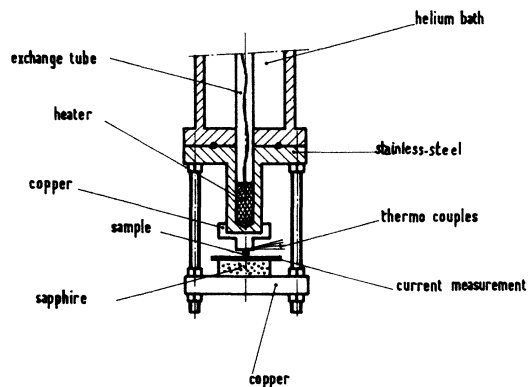


FIG. 1. Schematic diagram of the sample holder.

range ($T \lesssim 20$ °K) there is an electrical-field effect on the conductivity which is under investigation. The measurements reported in this paper are for a constant voltage low enough to avoid this effect. The electrical contacts are made by evaporating gold on two parallel rough faces because the thermal conduction across the gold-diamond interfaces is good enough for our purpose.¹⁹ It has been shown²⁰ that on rough or damaged surfaces the recombination velocity is high and exhibits carrier injection, resulting in reasonable ohmic contacts. The conductivity was independent of the direction of the current; electron irradiation studies (reported here and in Refs. 21–23) have demonstrated that the potential drop across the contacts was small compared with that across the bulk of the sample.

C. Measurements at high temperature

In the temperature range 350–1300 °K the conductivity measurements were performed in vacuum (10^{-6} Torr) to prevent surface graphitization of the samples. The sample is pressed between two molybdenum blocks. Electrical contacts are taken on tantalum sheets pressed between the sample faces and the blocks. One face of the sample is electrically insulated from the molybdenum by a thin alumina plate. A tantalum shield isolates the sample from the radiation of the oven.

D. Technique of measurement of the conductivity

The conductivity σ , at a given temperature, is strongly dependent upon the occupancy of the deep traps which are present in the samples. The samples contain boron dopant, partially compensated by a variety of traps at various levels in the forbidden gap associated with impurities and/or defects. The equilibrium occupancy of these traps and of the boron level depends on the temperature and on a possible external excitation. Since the

conductivity, especially in hopping regime, is very sensitive to a small change in occupancy of the boron impurity band, the measured values of σ will depend on the temperature T_e at which the thermal equilibrium was made and on the external excitation. When the sample is quenched to T_0 in order to measure σ at T_0 , the occupancy can still be the occupancy at T_e . Specifically, in thermal equilibrium at 0°K, all traps P_1, P_2, P_3, \dots , in concentrations $N_{D1}, N_{D2}, N_{D3}, \dots$, compensate the boron impurities; the concentration of the uncompensated boron is $N_A - N_{D0}$ where: $N_{D0} = N_{D1} + N_{D2} + N_{D3} + \dots$ and the conductivity is $\sigma(N_A, N_{D0})$. At temperature T , for which the traps P_1 are thermally excited, the concentration of the uncompensated boron is $N_A - N_D$ with $N_D = N_{D2} + N_{D3} + \dots$ and the conductivity is $\sigma(N_A, N_D)$. Moreover, ionizing irradiation, which creates electron-hole pairs, induces a change in the population distribution, decreasing the compensation. At low enough temperature, this metastable state is frozen: σ after ionizing irradiation (electron or x-ray irradiations, uv illumination) is different from σ at thermal equilibrium at the same temperature (not taking into account the introduction of defects). When the temperature is raised, electrons can be thermally released from some of the traps and, consequently, change σ .²⁴

Note that the results obtained for σ at a given temperature, presented in Sec. III, can be different depending upon the conditions in which they are taken. Measurements in the low-temperature range were taken after the samples had been quenched from 320°K before irradiation [to prevent the results being perturbed by the thermal release of carriers from traps which occurs at 160, 230, and 300°K (Ref. 24)] and from 250°K after irradiation [to prevent the defects created from annealing since the first annealing stage occurs at 270°K (Ref. 22)]. Measurements in the high-temperature range were taken with the sample in thermal equilibrium.

III. EXPERIMENTAL RESULTS

The variation of conductivity with temperature for the different samples studied is given in Fig. 2 for the low-temperature range and in Fig. 3 for the high-temperature range. The discrepancy between values of σ corresponding to the same temperature, in Fig. 2 and Fig. 3, is due, as explained in Sec. II D, to the fact that the occupancy of the traps is not the same for the low-temperature-range measurements or the high-temperature-range measurements. Moreover, we observed that heating of some of the samples around 1000°K induced permanent changes of σ , indicating that the

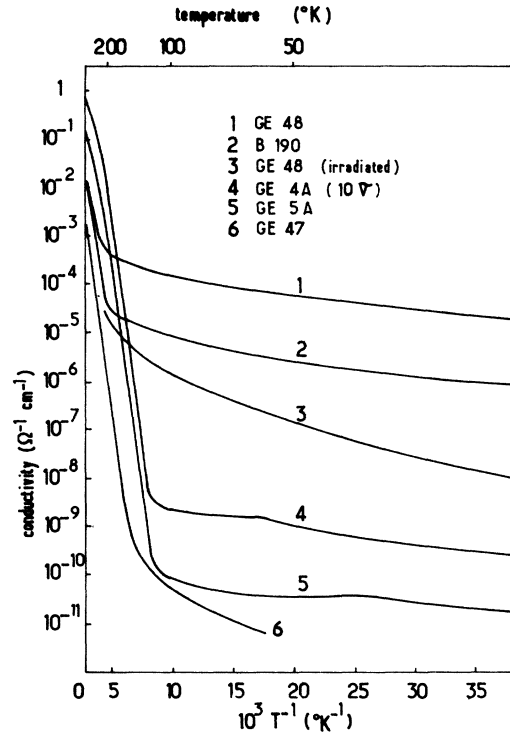


FIG. 2. Conductivity vs $10^3/T$ of various samples in the low-temperature range. Curve 3 corresponds to sample GE 48 having received an irradiation with 8×10^{16} electrons cm^{-2} at 0.7 MeV.

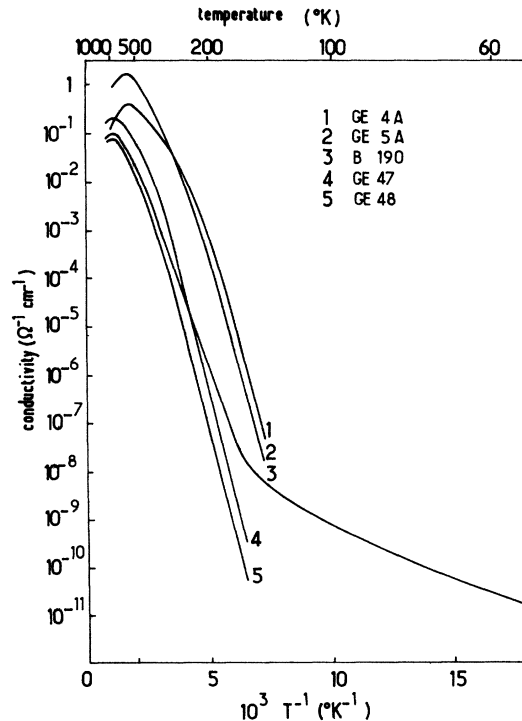


FIG. 3. Conductivity vs $10^3/T$ of various samples in the high-temperature range.

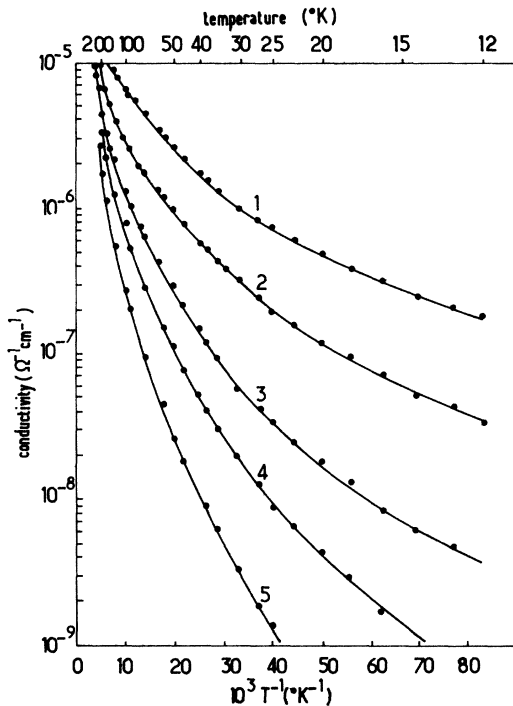


FIG. 4. Conductivity vs $10^3/T$ in sample GE 48 (the sample having been already irradiated and annealed); 1, before irradiation; 2, irradiated with 0.7-MeV electrons at a total dose of $2 \times 10^{16} \text{ cm}^{-2}$; 3, $4 \times 10^{16} \text{ cm}^{-2}$; 4, $6 \times 10^{16} \text{ cm}^{-2}$; 5, $8 \times 10^{16} \text{ cm}^{-2}$.

annealing of some defects had taken place at this temperature. For instance, at 200°K the conductivity of sample B 190 is about $10^{-6} \Omega^{-1} \text{ cm}^{-1}$ in Fig. 2 (low-temperature-range measurements) and about $10^{-5} \Omega^{-1} \text{ cm}^{-1}$ in Fig. 3 (high-temperature range measurements). All measurements in the low-temperature range were made prior to measurements in the high-temperature range.

Figure 4 shows the variation of σ vs T^{-1} for sample GE 48 with successive doses of 0.7-MeV electrons; each irradiation, performed below 20°K , is followed by heating at 230°K before measurements are taken (see Sec. IID).

IV. DETERMINATION OF N_A AND N_D

Boron has now been recognized as being the dominant acceptor in diamond.^{2,25} But the determination of bulk boron content in diamond has been difficult. Nuclear activation² and capacitance techniques^{25,26} give boron concentrations corresponding to a depth of a few microns, and for many crystals with a uniform boron acceptor content, one can infer an average bulk acceptor content for the crystal. A recently developed activation technique²⁷ appears to be capable of determining bulk boron contents of diamond. We

have attempted to determine N_A and N_D indirectly in two ways: (a) from electrical results using a graphical method, and (b) from the correlation between optical-absorption measurements and electrical measurements.

A. Graphical method

This method gives approximate solutions in different temperature ranges for the relation between the concentration of holes in the valence band p and N_A and N_D :

$$p \frac{N_D + p}{N_A - N_D - p} = \left(\frac{2\pi m^* kT}{h^2} \right)^{3/2} \exp\left(\frac{-E_A}{kT}\right). \quad (1)$$

Because of the geometry of the samples, their sizes, and the difficulty of realizing small electrical contacts, the variation of $p(T)$ is deduced from the variation of $\sigma(T)$. For this we need to know the hole mobility μ and the effective mass m^* between 600 and 1300°K .

In the temperature range 400 – 1000°K , μ is dominated by phonon scattering. Since a theoretical estimation could not be accurate (the concentration and the nature of the ionized centers is unknown), we used values which have been experimentally determined in similar samples. Dean *et al.*²⁸ found that μ , probably dominated by optical phonon scattering, varies as $T^{-2.8}$ in the temperature range 400 – 1000°K . We extrapolated μ in the range 1000 – 1300°K . The effective mass is taken to be equal to the electron mass m , because this is approximately the value found in Ref. 28.

According to Lee,²⁹ one can obtain N_A and N_D from the $\ln p$ -vs- T^{-1} curve in the following way. At the extrapolated value of the p -vs- T^{-1} curve, draw a line parallel to the temperature axis. This value of p is $p_1 = N_A - N_D$. At the point of intersection of this line and the linear extrapolation of the low-temperature part of the p -vs- T^{-1} curve,

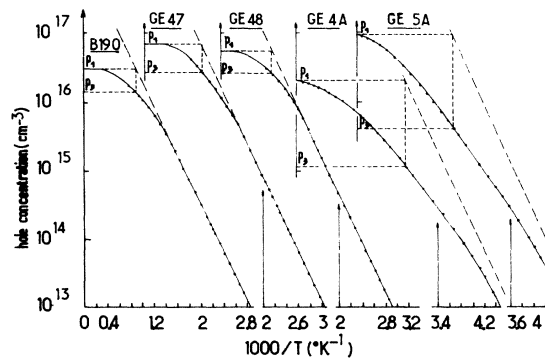


FIG. 5. Hole concentration vs $10^3/T$ and determination of p_1 and p_3 .

TABLE I. Determination of N_A and N_D (cm^{-3}) from the graphical method.

Sample	$N_A - N_D$	N_A	N_D	$K = N_D/N_A$
B 190	3×10^{16}	1.3×10^{17}	1×10^{17}	77%
GE 47	7×10^{16}	1.2×10^{17}	5×10^{16}	44%
GE 48 ^a	5.5×10^{16}	2.8×10^{17}	2.2×10^{17}	80%
GE 4A	2×10^{16}	2×10^{16}	5×10^{13}	0.3%
GE 5A	9×10^{16}	9×10^{16}	2×10^{14}	0.2%

^a Measurements in this sample have been performed after it had already received a series of electron irradiations.

draw a line parallel to the p axis. This line intersects the experimental curve at a hole concentration p_3 , where $p_3 = N_D^{1/2}(N_A^{1/2} - N_D^{1/2})$. Hence, p_1 and p_3 are obtained from graphical construction and then N_A and N_D are calculated from the following expressions:

$$N_A = (p_1 - p_3)^2 / (p_1 - 2p_3), \quad (2)$$

$$N_D = p_3^2 / (p_1 - 2p_3). \quad (3)$$

The graphical constructions are shown on Fig. 5 and the results are given in Table I.

B. Optical and electrical method

By combining optical absorption at 0.348 eV with Hall-effect and electrical-resistivity measurements, it has been established^{3,30} that a quantitative correlation exists between the intensity of this absorption band and the concentration $N_A - N_D$. We have also made electrical measurements at the same temperature (room temperature) to obtain the hole concentration

$$p = \frac{N_A - N_D}{N_D} \left(\frac{2\pi m^* kT}{\hbar^2} \right)^{3/2} \exp\left(\frac{-E_A}{kT}\right). \quad (4)$$

From these two measurements we deduced N_A and N_D . The results obtained are summarized in Table II. (Optical-absorption measurements have not been performed on Ge 4A and Ge 5A samples.)

C. Discussion of the results

There is an order-of-magnitude differences between the results obtained by the two methods. This is due to several factors. First, there are

permanent changes which have been induced by the thermal treatment at 1300 °K performed with the graphical method (after all the other measurements were done); these permanent changes correspond to the annealing of defects, i.e., to a decrease of N_D (compare Tables I and II). Second, the value of N_D obtained at high temperature (graphical method) is, as we explained in Sec. IID, different than the value obtained at moderate temperature (optical method) since more of the deep compensating levels are ionized at high temperature. This explains why the values of N_D , deduced from the graphical method, are smaller than the values deduced from the optical method. Finally, the results are only approximate since the values taken for μ and m^* are best estimates from published data.

We shall use the values given in Table II, when available, to calculate the parameters of the conduction σ at low temperature because the optical method corresponds to experimental conditions closer to the results taken at low temperature and also because these low-temperature measurements were performed prior to the permanent changes of σ which occurred at high temperature. For the samples for which no optical measurements were made (GE 4A and GE 5A) we shall use the values given in Table I.

V. DISCUSSION OF THE RESULTS

The slope S of $\ln \sigma$ vs T^{-1} changes abruptly in the range 150–200 °K (Fig. 2), where there is a transition from a conduction in the valence band (corresponding to a constant value of S) to a hopping

TABLE II. Determination of N_A and N_D (cm^{-3}) from optical measurements.

Sample	$N_A - N_D$	N_A	N_D	$K = N_D/N_A$
B 190	2.5×10^{17}	1.5×10^{18}	1.25×10^{18}	83%
GE 47	1.2×10^{17}	3.6×10^{17}	2.4×10^{17}	67%
GE 48	6.5×10^{16}	1.69×10^{18}	1.62×10^{18}	96%

regime. Indeed, the abrupt change in σ is not due to an artifact, such as a change from a bulk conductivity to a surface conductivity: the irradiation with successive doses of energetic electrons, which creates defects in the bulk, modifies σ in a regular fashion (Fig. 4).

The probability that a carrier hops from an occupied site to an unoccupied site, situated a distance R , depends on the overlap of the wave functions on the two sites and on the dispersion w in energy of the associated localized states. This probability is given by¹

$$P = \nu_{\text{ph}} \exp(-2\alpha R - w/kT), \quad (5)$$

where ν_{ph} is a factor depending on the phonon frequency, α^{-1} is the localization length characterizing the extension in space of the wave functions, and w is the energy difference between the two localized states. From the transition probability P , σ is calculated¹ using the Einstein relation (although this relation is valid only for nondegenerate systems) giving the mobility μ as a function of the diffusion coefficient D ($D/\mu = kT/e$, e is the electron charge; this theory apparently assumes that there is no problem concerning the definition of carrier mobility in a hopping regime). D is related to P through the relation: $D = f^{-1}PR^2$ (f is the coordination number; $f=6$ in diamond lattice). The number of carriers n participating in the hopping conduction consists of those which have an energy E such that $|E - E_F| < kT$. One therefore has $n = N_F kT$, where the density of states N_F at the Fermi level is given by

$$w = (3/4\pi)N_F R^3. \quad (6)$$

Then

$$\sigma = ne\mu = \frac{3e^2 f^{-1}}{4\pi} \frac{\nu_{\text{ph}}}{wR} \exp\left(-2\alpha R - \frac{w}{kT}\right). \quad (7)$$

A. Nearest-neighbor-hopping (NNH) regime

In the case where $w/kT \ll 2\alpha R$, P is maximum for R minimum: the carriers hop from one site to the nearest-neighbor site. Then the conductivity, occurring through thermally activated hops, is characterized by a constant activation energy ϵ_3 :

$$\sigma = \sigma_3 \exp(-\epsilon_3/kT). \quad (8)$$

The activation energy ϵ_3 is interpreted as being the energy necessary for the carrier to surmount the Coulomb potential which exists between the occupied and the unoccupied sites; it has been calculated by Miller and Abrahams³¹ by averaging all the possible values of w , in case of low compensation

$$\epsilon_3 = 1.61 (e^2/\chi)N_A^{1/3}(1 - 1.35K^{1/3}). \quad (9)$$

Shklovskii *et al.*^{32, 33} have examined the cases of low and high compensation and deduced the following expressions. For low compensation,

$$\epsilon_3 = 0.99(e^2/\chi)N_A^{1/3}(1 - 0.3K^{1/4}). \quad (10)$$

This formula is slightly different than that of Miller and Abrahams, and is in better agreement with the experimental results of Fritzsche^{34, 35} and Shklovskii and Shlimak.³⁶ For high compensation ($1 - K < 1$),

$$\epsilon_3 = \nu_1 (e^2/\chi)N_A^{1/3}(1 - K)^{-1/3}. \quad (11)$$

ν_1 is a constant on the order of unity and χ is the dielectric constant.

For intermediate impurity concentrations and for certain values of the compensation, an intermediary activation energy ϵ_2 is observed experimentally, so that

$$\sigma = \sigma_2 \exp(-\epsilon_2/kT) + \sigma_3 \exp(-\epsilon_3/kT). \quad (12)$$

Several mechanisms have been proposed³⁷⁻⁴³ to explain this intermediary activation energy and the following formulas have been derived:

$$\epsilon_2 = I - 3(e^2/\chi)N_A^{1/3} \quad (13)$$

according to Mycielskii,⁴⁰

$$\epsilon_2 \approx \frac{1}{2}(I_0 - I) \quad (14)$$

according to Nishimura,⁴² and

$$\epsilon_2 = I - |(le^2\delta^2/\chi a^2)(a + \delta R) \exp(-\delta R/a)| \quad (15)$$

according to Mikoshiba.⁴⁴ The quantity I is the ionization energy of the neutral impurity, and

$$I_0 = -4\pi a^3(N_A - N_D)I \left(\frac{l + 16(4 + \delta)}{(2 + \delta)^2} \right), \quad (16)$$

where a is the Bohr radius, δ is the screening factor (for positively charged acceptors), and l is the number of nearest neighbors.

Results of the calculation of ϵ_2 and ϵ_3 , using the different formulas, are given in Table III. The formula of Miller and Abrahams, valid for $K \ll 1$, is only applicable to samples GE 4A and GE 5A. In these calculations, the values of N_A and K are those given in Table II (except for samples GE 4A

TABLE III. Calculated activation energies ϵ_2 (meV) and ϵ_3 (meV) in a NNH regime.

Sample	Formula for ϵ_3		Formula for ϵ_2		
	9	11	15	14	13
B 190		54	340	≥ 170	250
GE 47		27	370	≥ 185	314
GE 48		90	250	≥ 125	156
GE 4A	9	6.5	370	≥ 185	350
GE 5A	16	11	370	≥ 185	340

TABLE IV. Slope energy E_s (meV) of $\ln\sigma$ vs T^{-1} plot measured at different temperatures. Also given are E_A values for each sample.

Sample	E_A ^a	$E_s(140^\circ\text{K})$	$E_s(77^\circ\text{K})$	$E_s(40^\circ\text{K})$	$E_s(20^\circ\text{K})$
B 190 b	340 ± 10	20	10	7.5	2
c	340 ± 10	60	40	20	1
GE 47 b	370 ± 10	80	22
b	250 ± 10	19	9	6.5	2.5
c	370 ± 10	d
GE 4A b	370 ± 10	d	8	7	1
GE 5A b	370 ± 10	d	6	4	2

^a Measured in the linear portion typically between 200 and 400 °K.

^b Before thermal treatment at 1000 °C.

^c After thermal treatment at 1000 °C.

^d In these cases E_s at 140 °K is still E_A .

and GE 5A), and a is taken to be 3.5×10^{-8} cm (see Sec. I).

We observe for our experimental results that in the hopping range it is not easy to associate the plots $\ln\sigma$ vs T^{-1} with a slope ϵ_3 , or even with two slopes ϵ_2 and ϵ_3 (this is difficult to see of Fig. 2 because of the scale chosen, but is more readily seen on Fig. 4). To compare the calculated values of ϵ_2 and ϵ_3 with possible experimental ones we measured the slopes of $\ln\sigma$ vs T^{-1} at different temperatures (140, 77, 40, and 20 °K). The energies associated with these slopes E_s are given in Table IV. We see by comparing Tables III and IV that the experimental values of energy defined in this way are much smaller than the calculated ones. Moreover, we observed a dependence of the possible experimental activation energy on the compensation: the slope of $\ln\sigma$ vs T^{-1} increases with the irradiation, i.e., with K (see Fig. 4 and Table V); such a dependence is not foreseen in the theories of Mycielski and Mikoshiba. Only Nishimura's theory indicates an increase of ϵ_2 with K but ϵ_2 should always remain larger than $\frac{1}{2}E_A$. Actually, the activation energies we measured in the low-temperature hopping regime

TABLE V. Slope energy E_s (meV) measured at different temperatures after successive doses (cm^{-2}) of 0.7-MeV electrons in sample GE 48.

Curve of Fig. 4	Irradiation dose	$E_s(77^\circ\text{K})$	$E_s(40^\circ\text{K})$	$E_s(20^\circ\text{K})$
1	0 ^a	8	6	2.5
2	2×10^{16}	10	7.5	3.5
3	4×10^{16}	14	10.5	4.5
4	6×10^{16}	17	12	5.5
5	8×10^{16}	22	14	7.5

^a The sample had been already irradiated and annealed before this experiment was performed.

are always very low compared to $\frac{1}{2}E_A$. This can be seen in Table IV where the activation energies in the low-temperature regime (E_s) and higher-temperature regime (E_A) are given.

The evaluation of ϵ_3 is easier since it should correspond to the value of E_s at the lowest temperature; a comparison of the calculated values of ϵ_3 with $E_s(20^\circ\text{K})$ for the different samples shows that the observed values are also, in this case, very low compared to the calculated ones (Tables IV and V).

It can therefore be concluded that the experimental results do not agree, either qualitatively or quantitatively, with a model in which the conductivity occurs through a NNH mechanism even if we admit the existence of two different regimes separated by large transition regions.

B. Variable-range-hopping (VRH) regime

The absence of a constant activation energy associated with the conductivity suggests that it takes place through a variable-range-hopping (VRH) mechanism. When w/kT is not negligible compared to $2\alpha R$, i.e., at very low temperatures or when the dispersion in energy w is large enough, then the hopping probability is maximum when $2\alpha R + w/kT$ is minimum. This occurs¹ for

$$R = (9/8\pi\alpha N_F kT)^{1/4} \quad (17)$$

and

$$w = (3/4\pi)(\frac{9}{8}\pi\alpha kT)^{3/4} N_F^{-1/4}, \quad (18)$$

and the conductivity obeys Mott's law¹

$$\sigma = \sigma_0 \exp(-A/T^m), \quad (19)$$

with

$$A = 2.06(\alpha^3/kN_F)^{1/4} \quad (20)$$

and $m = \frac{1}{4}$.

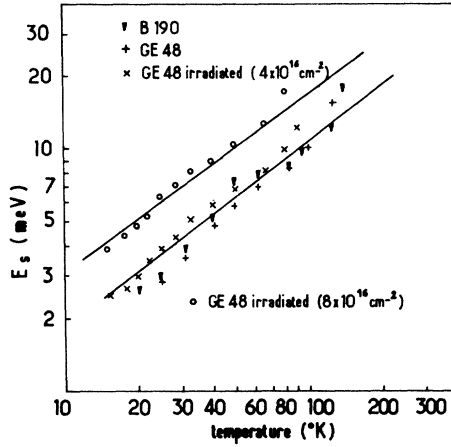


FIG. 6. Variation of E_s vs temperature for different samples, before and after irradiations.

This relation assumes a constant density of states N_F ; in case N_F is not constant, the relation is still valid,⁴⁵ with a value of m larger than $\frac{1}{4}$. In a VRH a mechanism, with N_F constant, the activation energy varies as $T^{3/4}$ [formula (18)]. We observe such a variation experimentally: E_s measured at various temperatures for unirradiated as well as irradiated samples is such that $\ln E_s$ varies linearly with $\ln T$ (Fig. 6) and the slope of $\ln E_s$ vs $\ln T$ is 0.75 ± 0.5 .

The conductivity follows Mott's law; this is shown on Fig. 7 for the unirradiated samples and

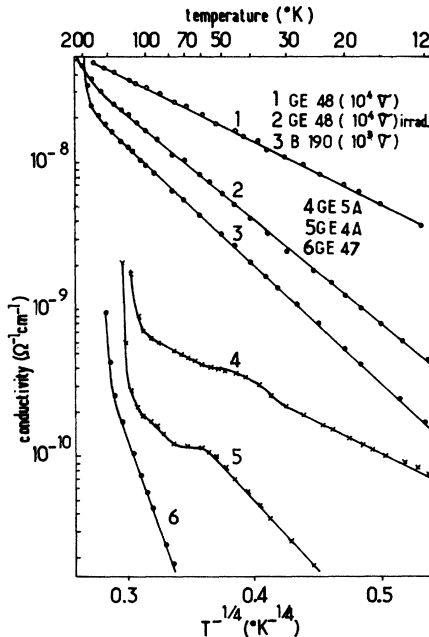


FIG. 7. Conductivity vs $T^{-1/4}$ for the different samples studied.

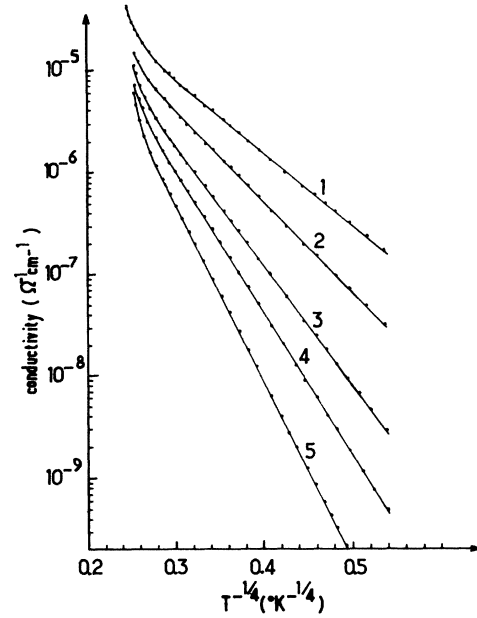


FIG. 8. Conductivity vs $T^{-1/4}$ for sample Ge 48 after successive electron irradiations. The number given on the curves correspond to those of Fig. 4.

on Fig. 8 for sample Ge 48 after successive doses of irradiation. Actually, it is difficult to determine the exact value of m since the dependence in T^{-m} becomes very small for $m < \frac{1}{3}$: on other words, the experimental results could also be adjusted with $m = \frac{1}{5}, \frac{1}{6}, \dots$ as well as $m = \frac{1}{4}$. It is therefore practically impossible to get a knowledge of the variation of N_F with the energy from the dependence of $\ln \sigma$ vs T^{-m} . In Fig. 9 we have plotted $\ln \sigma$ vs T^{-m} for $m = 1, \frac{1}{2}, \frac{1}{3},$ and $\frac{1}{4}$ for one sample just to show that the linear variation of $\ln \sigma$ with T^{-m} is indeed obtained only for $m \lesssim \frac{1}{4}$, i.e., that Mott's law appears to be operative.

How can the existence of the VRH mechanism be justified up to temperatures as high as 100–150 °K? The critical temperature T_c , at which the VRH mechanism becomes operative (i.e., the temperature at which w/kT is not negligible compared to $2\alpha R$), depends on the width of the impurity band and on the density of states at the Fermi level N_F . This critical temperature has been calculated by Shklovskii⁴⁶ who gave the following approximative expressions for $K \ll 1$:

$$T_c = e^2 N_A^{2/3} K^{1/3} / \chi K \alpha, \quad (21)$$

and for $K > 0.5$:

$$T_c = e^2 N_A^{2/3} / \chi K \alpha. \quad (22)$$

Because the boron level is deep in the forbidden gap ($E_A = E_V + 0.37$ eV), the free carrier concentration is negligible for temperatures 100–200 °K;

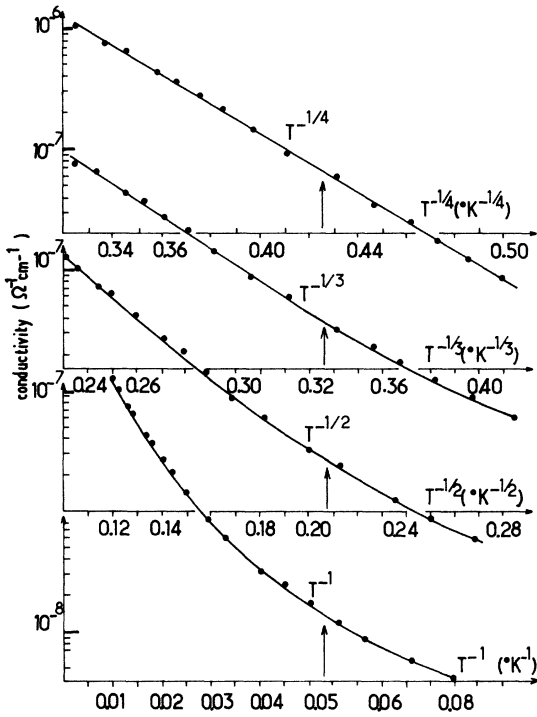


FIG. 9. Conductivity vs T^{-m} with $m=1, \frac{1}{2}, \frac{1}{3}$, and $\frac{1}{4}$ for sample Ge 48 irradiated with $4 \times 10^{16} \text{ cm}^{-2}$ electrons of 0.7 MeV.

because the Bohr radius for the fundamental state of the boron (acceptor) impurity is small ($\sim 3 \times 10^{-8} \text{ cm}$), it is possible to get nonmetallic conduction with impurity concentrations as high as 10^{18} – 10^{20} cm^{-3} . For such concentrations, the width w of the impurity band can be very large compared to kT even at 100–200 °K so that w/kT is not negligible compared to $2\alpha R$. This quantity w can be estimated, assuming it is caused by the Coulombic interaction between ionized impurities (separated by a distance r): $w = e^2/\chi r$; it varies between 20 and 200 meV for concentrations from 10^{17} to 10^{20} cm^{-3} when a 50% compensation is assumed.

Now that the analysis has indicated which hopping mechanism is operative, we can attempt a quantitative comparison with the theory using the values of the impurity concentration and of the compensation obtained in Sec. IV.

VI. QUANTITATIVE COMPARISON WITH THE THEORY

A. Density of states at the Fermi level

The theory of VRH has been developed¹ assuming a constant density of states in a region extending to several kT around the Fermi level. This is justified when the temperature range in which the

TABLE VI. Density of states at the Fermi level N_F ($\text{cm}^{-3} \text{ eV}^{-1}$) calculated using Shlovskii's formulas, slope A , ($^\circ\text{K}^{1/4}$) calculated, and experimentally measured from $\ln \sigma$ vs $T^{-1/4}$ curves.

Sample	N_F	A calculated ^a	A measured
B 190 ^b	9.5×10^{18}	40	18
GE 47 ^c	2.8×10^{18}	55	80
GE 48	8.8×10^{18}	42	58
GE 4A	1.7×10^{16}	203	21
GE 5A	3.4×10^{16}	172	10

^a Calculated using $\alpha^{-1} = 2 \times 10^{-7} \text{ cm}$.

^b Before thermal treatment at 1000 °C.

^c After thermal treatment at 1000 °C.

VRH mechanism is operative is small (such as in the case of crystalline germanium or silicon), or when the states are uniformly distributed (such as in amorphous materials). The density of states at the Fermi level N_F is then estimated as being the ratio of the concentration of the states to the width of the impurity band w ,

$$N_F \approx N_A/w = N_A \chi R / e^2. \quad (23)$$

The concentration of the ionized centers and R vary with the degree of compensation K ; Shklovskii,⁴⁶ to account for the variation of N_F with K , has given the following approximate formulas:

for $K \ll 1$,

$$N_F \approx (2\chi/e^2)N_D N_A^{-1/3}; \quad (24)$$

for $K \sim 0.5$,

$$N_F \approx (2\chi/e^2)N_A^{2/3}; \quad (25)$$

for $1 - K \ll 1$,

$$N_F \approx (2\chi/e^2)N_A^{2/3}(1-K)^{4/3}. \quad (26)$$

Results of the calculation of N_F for the different samples are given in Table VI.

B. Slope A of $\ln \sigma$ -vs- $T^{-1/4}$ curves

The experimental values of A , given in Table VI, have been plotted versus N_F in Fig. 10 (the error bars take into account the uncertainty in N_F). The calculated values of A (through the formula given in Sec. VB) cannot account for the experimental values when α^{-1} is taken to be the Bohr radius ($a = 3.5 \times 10^{-8} \text{ cm}$) as shown by curve 1. We have to consider a value of $\alpha^{-1} \approx 2 \times 10^{-7} \text{ cm}$ ($\pm 1 \times 10^{-7} \text{ cm}$) to get a satisfactory agreement (curve 2) between theory and experiment for samples B 190, GE 47, and GE 48. The results obtained with samples GE 4A and GE 5A would necessitate an even larger value of α^{-1} .

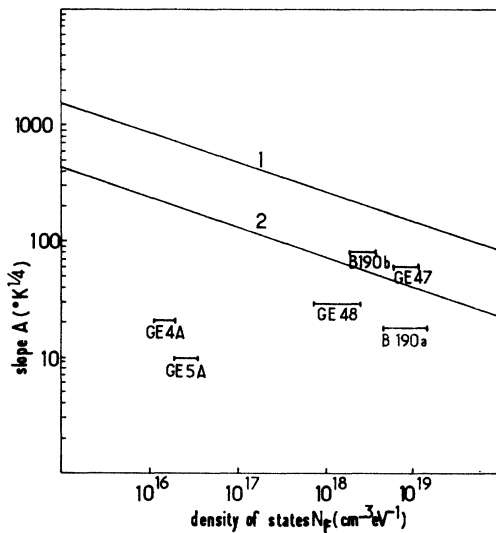


FIG. 10. Variation of the slope A of $\ln\sigma$ vs $T^{-1/4}$ with the density of states at the Fermi level N_F . Curve 1 is calculated with $\alpha^{-1} = 3.5 \times 10^{-8}$ cm and curve 2 with $\alpha^{-1} = 2 \times 10^{-7}$ cm.

This suggests that in these two samples either the evaluation of N_A and N_D we have made is wrong or the conduction mechanism, although of the same nature as in the other samples, occurs on impurity centers others than boron. This is supported by the fact that, in these two samples, N_A is very low, as well as K , compared to the other samples: N_F is very low and w very small and consequently it is difficult to conceive that the VRH regime occurs on boron centers for temperatures as high as 100°K. The fact that, in these samples, a kink in the $\ln\sigma$ -vs- $T^{-1/4}$ curve is observed (see Fig. 7) could be a manifestation of a change in the nature of the centers through which the conduction occurs. We therefore conclude that, in these two samples, the conduction occurs through VRH mechanism on another type of center, such as dislocations (as suggested by Mott). Indeed, as recalled in Sec. II A, the samples did have macroscopic inclusions and hence could very well contain a large concentration of dislocations.

Verification that a VRH mechanism is occurring can be made by studying the effect of an irradiation which changes the concentration of the compensating centers. The calculation of the variation of σ due to a variation ΔN_D in the concentration of the compensating centers, both for VRH and nearest-neighbor-hopping (NNH) cases is developed in Ref. 47 together with verifications of the formulas in cadmium telluride (for the NNH mechanism) and in diamond (for the VRH mechanism). It is shown that the introduction of a concentration ΔN_D of compensating centers, small compared to N_A and $N_A - N_D$, induces

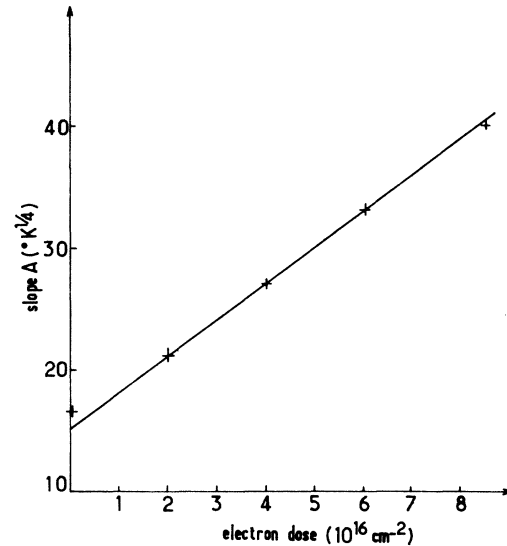


FIG. 11. Variation of the slope A (from $\ln\sigma$ -vs- $T^{-1/4}$ data) vs the dose of irradiation at 0.7 MeV for sample GE 48.

a variation of A that is linear with ΔN_D . The slopes A obtained after successive irradiations indeed vary linearly with the dose ϕ of irradiation (Fig. 11). Since the electrical conductivity measurements suggest the irradiation produce donor defects, the experimental data agree with prediction.

C. Critical temperature

It is difficult to obtain T_c . First, the formulas given by Shklovskii are only approximate. Second, it is experimentally difficult to determine precisely the transition temperature between the NNH and the VRH mechanisms and the larger T_c , the smaller the absolute accuracy. Nonetheless, one can attempt to determine T_c in two ways; first, by using the $\ln\sigma$ -vs- $T^{-1/4}$ plot (T_c is the temperature at which the conductivity no longer

TABLE VII. Estimated experimental and calculated critical temperatures T_c (°K).

Sample	Experiment		Theory c
	a	b	
B 190	~150	~120	80
GE 47	~120		31
GE 48	~170	~80	36

^a Temperature at which $\ln\sigma$ vs $T^{-1/4}$ is no longer linear.

^b Temperature at which E_s is no more proportional to $T^{3/4}$.

^c Calculated using $\alpha^{-1} = 2 \times 10^{-7}$ cm.

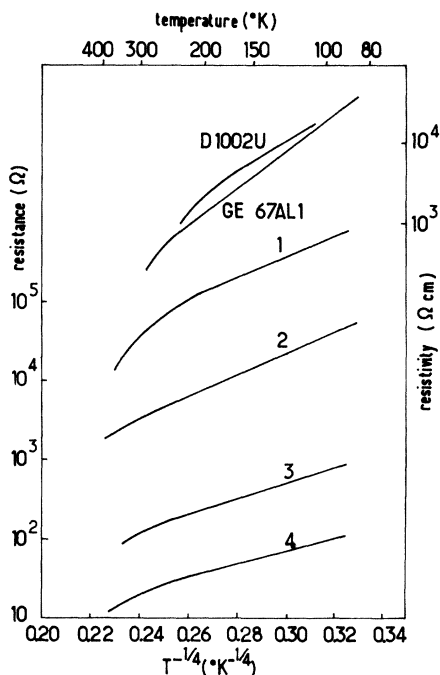


FIG. 12. Variation vs $T^{-1/4}$ of the resistivity in samples (D 1002 V and Ge 67 AL1) of Williams *et al.* (Ref. 12) and of the resistance in samples (1, 2, 3, and 4) of Tsay *et al.* (Ref. 13).

follows Mott's law); second, by using the E_s -vs- $T^{3/4}$ plot (T_c is the temperature at which E_s ceases to vary linearly with T). The experimental and calculated values of T_c are shown in Table VII. The second experimental method provides lower values of T_c , which are therefore closer to the values evaluated from the calculation. Considering the uncertainty in the experimental values of T_c and in the parameter α^{-1} , we consider the agreement with the theory satisfactory.

D. Analysis of previously published results

In the previously published results^{4,10-13} concerning the variation of conductivity in semiconducting diamonds, the hopping conductivity covers a relatively reduced temperature range ($1000/T$ varies from 3 to 10, while in our results $1000/T$ varies from 8 to 85). It was therefore difficult for the authors of these previous works to analyze fully the hopping regime; Williams *et al.*¹² noted that they needed two activation energies ($\epsilon_2 = 89$

meV and $\epsilon_3 = 32$ meV) to account for the shape of their curves $\ln\sigma$ vs T^{-1} ; they also noted that for one sample (GE 67 AL 1) $\ln\sigma$ was linear with $T^{-1/4}$. In Fig. 12 we show that Mott's law is valid for two samples of Williams *et al.*¹² and all of the samples of Tsay *et al.*¹³ This observation is, of course, insufficient to determine the mechanism for conduction; we simply note that the value of ϵ_2 proposed in Ref. 12 is very likely too small (see Table III) and that most probably the VRH mechanism is operative in these samples. Unfortunately, it is impossible to make a quantitative comparison of these results with the theory because the concentration of boron, as well as the compensation, are unknown. The values of N_A and N_D given by Williams *et al.*¹² have been estimated assuming that the acceptor impurity was aluminum.^{10,12,48,49} Later, it was demonstrated (by activation analysis measurements²) that the acceptor impurity was boron, and the authors themselves repudiated these values.³⁰

V. CONCLUSION

The boron concentration in samples B 190, GE 47, and GE 48, and the degree of compensation, lead one to expect conductivity will occur through a variable-range hopping mechanism at temperatures as high as 100–150 °K. We have shown that the results find their best explanation in terms of this regime of conduction since (a) it is not possible to define a constant activation energy (characteristic of a nearest-neighbor hopping regime) even at the lowest temperature; (b) even if we admit a regime for the conduction characterized by two activation energies (ϵ_2 and ϵ_3), it is not possible to account theoretically for the experimental values of these activation energies; (c) the activation energy below ~ 150 °K follows a $T^{3/4}$ law as anticipated by the theory; the conductivity follows Mott's law, $\sigma = \sigma_0 \exp(-A/T^{1/4})$; the slope A follows correctly the relation given by the theory; (e) the variation of A with the concentration of additional compensating centers introduced by irradiation is as foreseen by the theory; and (f) the experimental values of the critical temperature (below which the variable-range hopping regime applied) are comparable to the calculated values. We also suggest that for samples studied in Refs. 12 and 13, the regime of conductivity below 150 °K is also the variable-range hopping regime.

*Permanent address: Dept. of Physics, University of Damascus, Damascus, Syria.

†Laboratoire associé au CNRS.

¹For a review on hopping conduction, see for instance,

N. F. Mott and E. A. Davies, *Electronic Processes in Non-Crystalline Materials* (Clarendon, Oxford, 1971), Chap. 6.

²R. M. Chrenko, Phys. Rev. B **7**, 4560 (1973).

- ³P. T. Wedepohl, Proc. Phys. Soc. Lond. B 70, 177 (1957).
- ⁴G. N. Bezrukov, V. P. Butuzov, N. N. Gerasimenko, L. V. Lezheiko, Yu. A. Litvin, and L. S. Smirnov, Sov. Phys. Semicond. 4, 587 (1970).
- ⁵J. C. Bourgoin, P. R. Brosious, Y. M. Kim, and J. W. Corbett, Philos. Mag. 26, 1167 (1972).
- ⁶F. R. Allen and C. J. Adkins, Philos. Mag. 26, 1027 (1972).
- ⁷O. V. Emelyanenko, D. N. Nasledov, E. I. Nikulin, and I. M. Timchenko, Sov. Phys. Semicond. 6, 192 (1972).
- ⁸R. Coates and E. W. J. Mitchell, J. Phys. C 5, L113 (1972).
- ⁹W. B. Wilson, Phys. Rev. 127, 1549 (1962).
- ¹⁰E. C. Lightowers and A. T. Collins, Phys. Rev. 151, 685 (1966).
- ¹¹W. B. Wilson, Phys. Rev. 127, 1549 (1962).
- ¹²A. W. S. Williams, E. C. Lightowers, and A. T. Collins, J. Phys. C 3, 1727 (1970).
- ¹³Y. F. Tsay, K. P. Ananthanarayanan, P. J. Gielisse, and S. S. Mitra, J. Appl. Phys. 43, 3677 (1972).
- ¹⁴C. D. Clark, J. Kemmey, and E. W. J. Mitchell, Discuss. Faraday Soc. 31, 96 (1961).
- ¹⁵R. M. Chrenko, Nature (London), Phys. Sci. 229, 165 (1971).
- ¹⁶H. M. Strong and R. M. Chrenko, J. Phys. Chem. 75, 1838 (1971).
- ¹⁷F. P. Bundy, J. Chem. Phys. 38, 631 (1963).
- ¹⁸J. Bourgoin, J. Zizine, S. Squelard, and P. Baruch, Radiat. Eff. 2, 287 (1970).
- ¹⁹R. J. Caveney, S. E. Jenkins, and G. Ziudema, Diamond Research (Industrial Diamond Information Bureau, London, 1971), p. 20.
- ²⁰A. T. Collins, E. C. Lightowers, and A. W. S. Williams, in Ref. 19, 1970, p. 19.
- ²¹J. C. Bourgoin and B. Massarani, Phys. Rev. B 14, 3690 (1976).
- ²²B. Massarani and J. C. Bourgoin, Phys. Rev. B 14, 3682 (1976).
- ²³J. C. Bourgoin, B. Massarani, and R. Visocekas, Phys. Rev. B (to be published).
- ²⁴The study of these traps, using thermally activated conductivity and thermoluminescence, is the subject of Ref. 23.
- ²⁵E. C. Lightowers and A. T. Collins, J. Phys. D 9, 951 (1976).
- ²⁶G. H. Glover, Solid State Electron. 16, 973 (1973).
- ²⁷J. P. F. Sellschop, D. M. Bibby, R. J. Kiddy, D. W. Mingay, and M. J. Renan, 1975, Diamond Conference, Cambridge (unpublished).
- ²⁸P. J. Dean, E. C. Lightowers, and D. R. Wright, Phys. Rev. 140, A352 (1965).
- ²⁹P. A. Lee, Br. J. Appl. Phys. 8, 340 (1957).
- ³⁰A. T. Collins and A. W. S. Williams, J. Phys. C 4, 1789 (1971).
- ³¹A. Miller and E. Abrahams, Phys. Rev. 120, 745 (1960).
- ³²B. I. Shklovskii, A. L. Efros, and I. Y. Yanehef, JETP Lett. 14, 233 (1971).
- ³³B. I. Shklovskii, A. L. Efros, and I. Y. Yanehef, Phys. Status Solidi 50, 45 (1972).
- ³⁴H. Fritzsche, J. Phys. Chem. Solids 6, 69 (1958).
- ³⁵H. Fritzsche, Phys. Rev. 99, 406 (1955).
- ³⁶B. I. Shklovskii and I. S. Shlimak, Sov. Phys. Semicond. 6, 104 (1972).
- ³⁷N. F. Mott and W. D. Twose, Adv. Phys. 10, 107 (1961).
- ³⁸H. Fritzsche and K. Lark-Horovitz, Phys. Rev. 113, 999 (1959).
- ³⁹H. Fritzsche and M. Cuevas, Phys. Rev. 119, 1238 (1960).
- ⁴⁰J. Mycielski, Phys. Rev. 122, 99 (1961).
- ⁴¹C. Yamanouchi, J. Phys. Soc. Jpn. 18, 1775 (1963).
- ⁴²H. Nishimura, Phys. Rev. 138, A815 (1965).
- ⁴³F. H. Pollak, Phys. Rev. 138, A18 (1965).
- ⁴⁴Cited in Ref. 43.
- ⁴⁵M. Pollak, J. Non-Cryst. Solids 8-10, 486 (1972); and 11, 1 (1972).
- ⁴⁶B. I. Shklovskii, Sov. Phys. Semicond. 6, 1053 (1973).
- ⁴⁷B. Massarani, M. Caillot and J. C. Bourgoin, Phys. Rev. B 15, 2224 (1977).
- ⁴⁸I. G. Austin and R. Wolf, Proc. Phys. Soc. Lond. B 69, 329 (1956).
- ⁴⁹P. J. Dean, Phys. Rev. 139, 1588 (1965).